J. Fluid Mech. (2002), *vol.* 453, *pp.* 289–313.
DOI: 10.1017/S0022112001006905 Printed in the United Kingdom

Generation of sound and instability waves due to unsteady suction and injection

By XUESONG WU

Department of Mathematics, Imperial College, 180 Queens Gate, London SW7 2BZ, UK

(Received 3 January 2001 and in revised form 12 September 2001)

This paper analyses the generation of sound and Tollmien–Schlichting (T–S) waves in a compressible boundary layer that is subject to unsteady suction and injection. An asymptotic approach based on the triple-deck formulation has been developed to calculate the sound field. It is shown that in addition to the three familiar asymptotic regions that govern the near-field hydrodynamic motion, an extra outer region controlling the sound radiation must be introduced. The near-field solution is sought via an asymptotic expansion in ascending powers of $\epsilon = R^{-1/8}$, where R is the global Reynolds number. The first three terms in the asymptotic series are found to act as quadrupole, dipole and monopole sources respectively, and make equal order-of-magnitude contributions to the acoustic far field. The analysis also allows the amplitude of the excited T–S waves to be determined to $O(\epsilon)$ accuracy. It is believed that the flow structure and solution procedure may be used to solve a range of aeroacoustic problems.

1. Introduction

The present study is concerned with the two important processes that take place simultaneously when a subsonic compressible boundary layer is subject to time-periodic suction and injection, namely generation of instability, i.e. Tollmien–Schlichting (T–S) waves, and radiation of sound to the far field. This problem will be used as a prototype flow to develop an asymptotic procedure for calculating the sound radiation in a shear flow, and to clarify the role of instability waves in sound generation. The problem itself is of practical relevance since unsteady suction/injection has been used as an actuator in some laminar-flow control techniques (such as micro-electro-mechanical devices), where a suitable suction may excite T–S waves to cancel the oncoming naturally occurring T–S waves generated by the free-stream turbulence. Such unsteady suction/injection is often referred to as a synthetic jet in the field of flow control. For brevity, in the rest of the paper we shall omit 'injection' on the understanding that the suction velocity can be both positive and negative.

Usually the streamwise extent of suction is fairly localized and in no case exceeds the wavelength of the T–S waves. Thus in a suitable frequency range, the unsteady suction alone is capable of directly exciting T–S waves, whose magnitude would be proportional to the suction strength. The problem was first analysed by Gaster (1965) and more recently by Ashpis & Reshotko (1990) on the basis of the Orr–Sommerfeld equation, and formal solutions were given for the boundary-layer response. Terent'ev (1981, 1984) formulated the same problem in the framework of triple-deck theory and obtained the leading-order approximation to the T–S wave amplitude. Bodonyi

& Duck (1992) investigated the control of T–S waves by unsteady suction over the triple-deck scale. The same approach will be employed in the present study, but we shall determine the amplitude of the T–S waves up to $O(\epsilon)$ accuracy. Clearly, unsteady suction, being localized, generates T–S waves without involving a scale-conversion mechanism. This is unlike the boundary-layer receptivity to the unsteady disturbances in the free stream (i.e. the sound wave and convecting gust). Those disturbances can excite T–S waves only through mutual interaction (Wu 1999) or by interacting with certain rapidly varying streamwise inhomogeneities such as the mean-flow distortion induced by a local roughness (Goldstein 1985; Ruban 1984; Duck, Ruban & Zhikharev 1996). The magnitude of the excited T–S waves is thus proportional to the product of those of the two participating agents.

The more important aim of our study is to present an asymptotic approach which enables us to analyse, in a systematic and self-consistent manner, the sound radiation due to a source that is embedded in a shear flow and possibly associated with viscous motions. The effect of a mean shear flow on the sound radiation has long been an outstanding issue (see e.g. Ffowcs Williams 1977), and for that reason has been a subject of extensive study.

As is well known, the main theoretical tool for predicting the sound generated by unsteady and often turbulent fluid motions has been the acoustic analogy theory (Lighthill 1952). This theory is based on the fact that from the basic equations governing the fluid motion, an inhomogeneous wave equation can be derived for the density or pressure fluctuation. This equation is inherently nonlinear, but is in exact analogy with the conventional acoustic equation if the inhomogeneous term, which consists of the Reynolds as well as viscous stresses, is interpreted as the source acting on a fictitious medium. Now if the velocity is decomposed into a sum of mean and fluctuating parts, then the source will consist of the product of the mean-flow gradient with the fluctuation as well as the product of the fluctuation with itself. The role of the former term in sound generation was first considered by Lighthill (1954).

Subsequent investigations departed somewhat from Lighthill's thinking in that some of what he regarded as source terms were now viewed as describing the propagation of the sound and hence were moved to the left-hand side of the equation. This was the main idea underlining the formulation of more complex acoustic analogies (Phillips 1960; Lilley 1974; Howe 1975) which display explicitly the so-called sound–flow interaction, such as the convection and refraction effects. By rearranging the fundamental equations of fluid motion in different ways, each of these authors derived an equation for a quantity that represents the sound. In exact form, they are nonlinear, and so have to be linearized before meaningful calculations can be carried out.

Lilley's analogy has received considerable attention. In this approach, the inhomogeneous compressible Rayleigh equation, which is commonly referred to as Lilley's equation, takes the place of the wave equation in Lighthill's original theory. Thus Lilley's equation has the unique property that in the absence of any volume source, it describes the propagation of an infinitesimal sound wave through the mean flow. But whether or not this property makes Lilley's approach superior to other analogies has been a matter of debate, and indeed several objections to Lilley's approach have been raised (see e.g. Howe 1975; Ffowcs Williams 1977; Crighton 1981). On the other hand, Mani (1976) gave forceful arguments in favour of Lilley's equation. Analytical solutions to Lilley's equation are possible only for special profiles such as a plug-flow (i.e. vortex sheet) model, and these were worked out by Mani (1976). A justification for using the vortex-sheet model was provided by Ffowcs Williams (1974) and Dowling,

Ffowcs Williams & Goldstein (1978), who established an exact analogy between this idealized model and the real problem. For an arbitrary mean-flow profile, Lilley's equation has to be solved numerically, and a recent calculation is that of Tam (1998). At the low- and high-frequency limits, asymptotic solutions are possible and have been obtained by a number of authors. A review of these results can be found in Goldstein (1976, 1984*a*). Detailed comparisons with experiments on jet noise, such as were presented in Mani (1976) and Goldstein (1976, 1984*a*), indicate that Lilley's approach is able to capture many radiation features which are beyond the scope of Lighthill's classical theory. However, the mean-flow effect on the sound emission can be explicitly interpreted only when one assumes that the source is independent of the mean flow. Obviously this assumption cannot be true in most applications (e.g. the jet noise), where the acoustic source draws energy from the background shear flow.

The theories based on the idea of acoustic analogy have achieved considerable success. However they have a fundamental weakness, that is, the very entity of concern, the sound, is not defined in manner independent of the specific analogy. Rather, sound is taken to be some quantity which is put on the left-hand side of a wave-like equation, while the terms on the right-hand side are viewed as its source. This kind of distinction between sound and source is somewhat arbitrary, even though the well accepted analogies were based on the best physical intuitions. This arbitrariness of course does not matter at all as long as the analogy remains in the exact form. However, before any acoustic analogy can be used to calculate the absolute level of the sound, the source has to be evaluated in advance. That has to be done approximately because to do it exactly amounts to solving the complete equations governing the compressible flow. Then two questions arise: (*a*) how the source should be approximated, and (*b*) in what sense the sound calculated by a particular analogy is indeed an approximation to the true sound field. There have been no definitive or general answers to the above questions. A well-used approximation, advocated by Lighthill himself, is to solve the incompressible flow in a limited spatial domain. It was suggested that this scheme is valid for low-speed flows. A natural step to put it on a formal and quantitative basis is by systematic small-Mach-number asymptotic expansions. Such an attempt was made by Crow (1970) and Obermeier (1967). They found that the small-Mach-number assumption alone is insufficient for justifying Lighthill's approximation; for the latter to be valid the unsteady flow has to satisfy certain stringent conditions.

The work of Crow (1970) and Obermeier (1967) stimulated the development of the alternative approach to aeroacoustics based on the method of matched asymptotic expansion. The principal idea of this theory is as follows. Suppose that the sound is emitted by the motion of vortices, of size l_v say, contained in a domain of size $L \sim l_v$. If the typical velocity of the vortex motion is u, then its timescale is l_v/u and the emitted sound has the wavelength $\lambda_a \sim a(l_v/u)$, where a is the sound speed. In the small Mach number limit $M = u/a \ll 1$, $\lambda_a \gg l_v$, and two distinct asymptotic regions emerge: a hydrodynamic near field on the scale l_v, where the flow is incompressible to the leading-order approximation, and an acoustic far field on the scale λ_a, through which the energy leaked from the hydrodynamic motion propagates in the form of sound. This approach is particularly suited for calculating the acoustic radiation due to certain vortex motions, and a review of the work in this field was given by Kambe (1986), but the general idea has much wider applications in acoustics (Crighton 1972*a*, *b*; Crighton & Leppington 1971, 1973).

It is apparent that the asymptotic approach overcomes, at least for the problems that it can tackle, the inherent weakness of the acoustic analogy theory. First, the sound

is defined as the far field of the hydrodynamic motion. This unambiguous definition comes about mathematically, but is completely appropriate from the physical point of view. Secondly, the source is calculated explicitly, or at any rate the way in which it has been approximated is fully specified. In such an asymptotic approach, the determination of the unsteady flow that radiates the sound is a natural and integral part of the acoustic problem.

The asymptotic approach therefore appears to be a promising tool for studying the sound radiation due to a source surrounded by a shear flow. It is of course unrealistic at present to formulate a general theory. Instead, we shall focus on the situation where the unsteady source flow is governed by triple-deck structure. The particular problem that we choose, the subsonic compressible boundary layer subject to periodic suction, is perhaps the simplest of the kind. Mathematically, the problem has the advantage that it can be described and solved in a completely self-consistent manner by using the high-Reynolds-number asymptotic approach. There is no need to make any *ad-hoc* assumption. The problem has a number of novel aspects. First, all previous asymptotic theories of acoustic radiation almost invariably assume that the flow is nearly incompressible, i.e. the relevant Mach number is small. Such an assumption is not necessary for our problem, with the result that compressibility appears as a leading-order effect in the hydrodynamic near field. Secondly, the flow supports instability waves, which will eventually dominate the flow field sufficiently far downstream. But this leads to no indeterminacy since the amplitude of these waves is fully determined by the given conditions.

The rest of the paper is structured as follows. In § 2, the problem is formulated, and the relevant scalings are specified so that the boundary-layer response to the suction can be described by triple-deck theory. The linearized solution, which is possible when the suction velocity is less than $O(R^{-3/8})$, is sought in § 3, where R is the Reynolds number based on the distance of the suction from the leading edge. The solution in each deck can be expanded in ascending powers of $R^{-1/8}$, and the first three terms in the expansion are obtained. In § 4, the amplitude of the T–S wave is calculated to $O(\epsilon)$ accuracy. To determine the sound field, we examine in § 5.1 the large-distance asymptotic behaviour of the pressure in the upper layer. It is found that the first three terms in the solution contribute quadrupole, dipole and monopole sources respectively to the sound generation, indicating that the expansion in the upper layer becomes disordered in the far field. The pressure in this region, considered in § 5.2, is governed by the conventional acoustic equation in a uniformly moving medium, and its solution can be represented by a linear superposition of quadrupole, dipole and monopole, with the combination coefficients being determined by matching with the solution in the upper deck. The directivity of the radiated sound is examined. Further discussions are given in § 6.

2. Formulation and scalings

We consider the two-dimensional compressible boundary layer over a semi-infinite plate, which is subject to a localized suction at a distance l downstream the leading edge. The oncoming flow is assumed to be uniform with velocity U_∞. The mean density, temperature, viscosity and sound speed in the free stream are denoted by ρ_∞, T_∞, μ_∞ and a_∞ respectively. We define the Mach number

$$M = U_\infty / a_\infty,$$

and the Reynolds number

$$R = U_\infty l/v_\infty, \tag{2.1}$$

where $v_\infty = \mu_\infty/\rho_\infty$ is the kinematic viscosity. We shall focus on the subsonic flow with $M < 1$ being of $O(1)$. The Reynolds number is taken to be large.

The flow is to be described in a Cartesian coordinate system (x_1, x_2) whose origin is taken to be at the distance l from the leading edge, where x_1 and x_2 are along and normal to the plate, non-dimensionalized by l. The time variable t is normalized by l/U_∞. The velocity (u, v), density ρ, and temperature τ are non-dimensionalized by U_∞, ρ_∞ and T_∞ respectively, while the non-dimensional pressure p is introduced by writing the dimensional pressure as $p_\infty + \rho_\infty U_\infty^2 p$, where p_∞ is a constant.

For simplicity, the fluid is taken to be a perfect gas, with a constant ratio of specific heats, γ. The governing equations of the flow are

$$\frac{\partial \rho}{\partial t} + \nabla \cdot (\rho \boldsymbol{u}) = 0, \tag{2.2}$$

$$\rho \frac{\mathrm{D}\boldsymbol{u}}{\mathrm{D}t} = -\nabla p + \frac{1}{R}\nabla \cdot (2\mu \boldsymbol{e}) + \frac{1}{R}\nabla \left((\mu' - \tfrac{2}{3}\mu)\nabla \cdot \boldsymbol{u} \right), \tag{2.3}$$

$$\rho \frac{\mathrm{D}\tau}{\mathrm{D}t} = (\gamma - 1)M^2 \frac{\mathrm{D}p}{\mathrm{D}t} + \frac{1}{PrR}\nabla \cdot (\mu \nabla \tau) + \frac{(\gamma - 1)M^2}{R}\Phi, \tag{2.4}$$

$$1 + \gamma M^2 p = \rho \tau, \tag{2.5}$$

where $\boldsymbol{u} = (u, v)$, $\boldsymbol{e}$ and Φ represent the tensor of the strain rate and the dissipation function:

$$e_{ij} = \frac{1}{2}\left(\frac{\partial u_i}{\partial x_j} + \frac{\partial u_j}{\partial x_i} \right), \quad \Phi = 2\mu \boldsymbol{e} : \boldsymbol{e} + (\mu' - \tfrac{2}{3}\mu)(\nabla \cdot \boldsymbol{u})^2$$

and Pr is the Prandtl number. The operators such as ∇ are defined with respect to the variables (x_1, x_2). The shear viscosity μ is assumed to obey the Chapman viscosity law,

$$\mu = C\tau$$

where C is unity for the normalization adopted above, and so will drop out of the equations hereafter. The bulk viscosity μ' will play no role to the order of approximation (and is usually taken to be zero by Stokes' hypothesis).

Let us now define a boundary-layer variable $y = R^{1/2}x_2$ and write x_1 as x, i.e.

$$(x, y) = (x_1, R^{1/2}x_2).$$

The velocity profile of the unperturbed basic flow is given by

$$U_B = f'(\eta), \quad \text{where} \quad \eta = [(1 + x)]^{-1/2} \int_0^y R_B \, \mathrm{d}y,$$

with R_B being the mean density profile and f satisfying the Blasius equation

$$f'''(\eta) + \tfrac{1}{2} f f'(\eta) = 0.$$

As $y \to 0$,

$$U_B(y) \to \lambda (T_w/T_\infty)^{-1} y + \tfrac{1}{6}(\gamma - 1)M^2 \lambda^3 (T_w/T_\infty)^{-4} y^3 + O(y^4),$$

where T_w is dimensional temperature at the wall, and the local skin friction

$$\lambda = \lambda_0 (1 + x)^{-1/2} \quad \text{with} \quad \lambda_0 \approx 0.3321. \tag{2.6}$$

We shall assume that the wall is adiabatic and the Prandtl number Pr is unity. The temperature profile, $T_B(y)$, is then related to $U_B(y)$ via

$$T_B = 1 + \tfrac{1}{2}(\gamma - 1)M^2(1 - U_B^2).$$

Since $T_B R_B = 1$, it follows that

$$R_B \to (T_w/T_\infty)^{-1} + \tfrac{1}{2}(\gamma - 1)M^2\lambda^2(T_w/T_\infty)^{-4}y^2 + O(y^3).$$

It is worth mentioning that the analysis in the present paper can be easily generalized to a general viscosity law and an arbitrary Prandtl number. The assumptions of the Chapman law and unity Prandtl number are made simply to avoid some unnecessary complications which would otherwise be a distraction from the main issue.

Since the suction is periodic in time, we may write the total velocity field as a sum of the steady Blasius flow and a time-harmonic unsteady flow

$$(u, v, p, \rho, \tau) = (U_B, R^{-1/2}V_B, 0, R_B, T_B) + (\tilde{u}, \tilde{v}, \tilde{p}, \tilde{\rho}, \tilde{\tau})\mathrm{e}^{-\mathrm{i}\omega_s t} + \text{c.c.}, \tag{2.7}$$

with ω_s being the frequency of the suction. We are interested in the case where the suction velocity is small so that substitution of (2.7) into (2.2)–(2.5) yields the linearized Navier–Stokes equations, which to the required order of approximation can be written as

$$-\mathrm{i}\omega_s\tilde{\rho} + U_B\tilde{\rho}_x + R_B\tilde{u}_x + \epsilon^{-4}(R_B\tilde{v}_y + R_{B,y}\tilde{v}) = 0, \tag{2.8}$$

$$R_B\{-\mathrm{i}\omega_s\tilde{u} + U_B\tilde{u}_x + \epsilon^{-4}U_{B,y}\tilde{v}\} = -\tilde{p}_x + (T_B\tilde{u}_y)_y + (U_{B,y}\tilde{\tau})_y, \tag{2.9}$$

$$R_B\{-\mathrm{i}\omega_s\tilde{v} + U_B\tilde{v}_x\} = -\epsilon^{-4}\tilde{p}_y + (T_B\tilde{v}_y)_y, \tag{2.10}$$

$$\begin{aligned} R_B\{-\mathrm{i}\omega_s\tilde{\tau} + U_B\tilde{\tau}_x + \epsilon^{-4}T_{B,y}\tilde{v}\} &= (\gamma - 1)M^2\{-\mathrm{i}\omega_s\tilde{p} + U_B\tilde{p}_x\} \\ &\quad + (T_B\tilde{\tau}_y)_y + 2(\gamma - 1)M^2(T_B)U_{B,y}\tilde{u}_y, \end{aligned} \tag{2.11}$$

$$\gamma M^2\tilde{p} = T_B\tilde{\rho} + R_B\tilde{\tau}, \tag{2.12}$$

where we have defined the small parameter

$$\epsilon = R^{-1/8}.$$

In (2.8)–(2.11), we have ignored (a) the terms involving V_B or the streamwise derivatives of the mean-flow quantities (such as $U_{B,x}$, $T_{B,x}$ etc.), (b) the momentum and temperature diffusion in the streamwise direction, and (c) all the terms in the dissipation function except the leading-order one. The temperature perturbation $\tilde{\tau}$ can be eliminated among (2.8), (2.11) and (2.12) to give

$$(-\mathrm{i}\omega_s\tilde{\rho} + U_B\tilde{\rho}_x) + \epsilon^{-4}R_{B,y}\tilde{v} = R_BM^2(-\mathrm{i}\omega_s\tilde{p} + U_B\tilde{p}_x) + T_B^2\tilde{\rho}_{yy} - 2(\gamma - 1)M^2U_{B,y}\tilde{u}_y. \tag{2.13}$$

Equation (2.9) can be rewritten, on replacing $\tilde{\tau}$ using the state equation (2.12), as

$$R_B\{-\mathrm{i}\omega_s\tilde{u} + U_B\tilde{u}_x + \epsilon^{-4}U_{B,y}\tilde{v}\} = -\tilde{p}_x + (T_B\tilde{u}_y)_y + \left(U_{B,y}T_B(\gamma M^2\tilde{p} - T_B\tilde{\rho})\right)_y. \tag{2.14}$$

Equations (2.8), (2.10), (2.13) and (2.14) form the system governing the four quantities $(\tilde{u}, \tilde{v}, \tilde{p}, \tilde{\rho})$. It is subject to the boundary condition at the wall:

$$\tilde{u} = 0, \quad \tilde{v} = \tilde{v}_s(x) \quad \text{at} \quad y = 0.$$

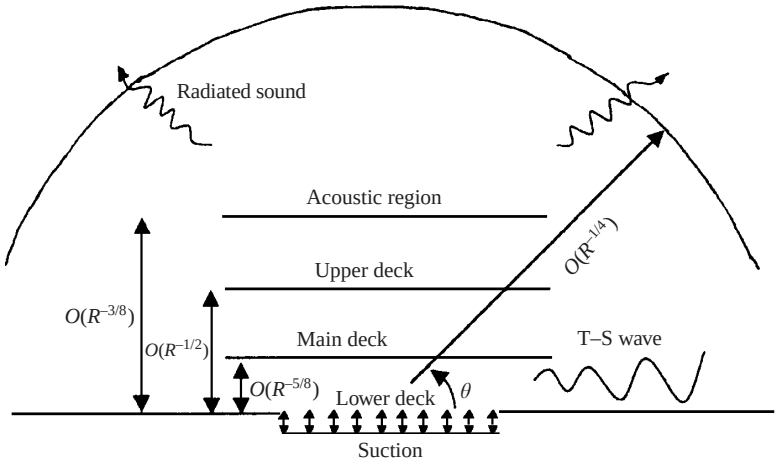

FIGURE 1. A sketch of the flow structure illustrating the radiation and receptivity processes.

To study the generation of T–S waves and the acoustic radiation, we shall perform an asymptotic analysis based on the triple-deck formalism. For this approach to be applicable, the frequency and the streamwise extent of the suction are assumed to be of $O(R^{2/8})$ and $O(R^{-3/8})$ respectively. For a linearized analysis to be valid, we must assume that

$$v_s \ll O(R^{-3/8}).$$

As far as calculating the sound at the fundamental frequency ω_s is concerned, the above condition is sufficient. However, nonlinear interaction generates harmonics, and so there may be radiation at frequencies $2\omega_s$, $3\omega_s$, etc. An interesting question is whether the sound with these tones can be as strong as the fundamental for some moderate-sized v_s. This issue is worth further investigation, but the sound at the harmonics is definitely negligible if $v_s \ll R^{-5/8}$, for which no harmonics appear in the expansion (2.7) to the required order.

It is convenient to introduce the faster time and spatial variables

$$\bar{t} = \epsilon^{-2}K^{-1}t, \quad \bar{x} = \epsilon^{-3}K^{-1}x, \tag{2.15}$$

and write

$$\omega_s = \epsilon^{-2}K^{-1}\omega, \quad \tilde{v}_s = \epsilon^3(T_w/T_\infty)^{1/2}V_s(\bar{x}).$$

where $K = (T_w/T_\infty)^{3/2}$, and suitable renormalizations have been included for later convenience.

The unsteady flow is described by the standard triple-deck structure consisting of the lower, middle and upper decks. These three regions as a whole will be referred to as the hydrodynamic near field. It turns out that the expansion in the upper deck is not uniformly valid. An acoustic outer region with both the streamwise and transverse scales being $O(R^{-1/4})$ has to be introduced to describe the conversion of the hydrodynamic motion into the sound. The whole flow structure thus consists of four decks, as is illustrated in figure 1. Note that for $M = O(1)$ the sound has a wavelength of $O(R^{-1/4})$, which is much larger than the $O(R^{-3/8})$ size of the source, and so the source is always compact regardless of the Mach number; there is no need to assume the Mach number to be small.

Strictly speaking, the governing equations have coefficients that vary with x. Fortunately, under the condition that $R \gg O(1)$ such an x-variation is purely parametric,

and in fact is so slow that its effect does not appear to the required order of approximation in this study. The equations can be solved by taking the Fourier transform with respect to $\bar{x}$. Let $\widehat{V}_s(k)$ denote the Fourier transform of $V_s(\bar{x})$. Then

$$\widehat{V}_s(k) = \frac{1}{(2\pi)^{1/2}} \int_{-\infty}^{\infty} V_s(\bar{x}) \mathrm{e}^{-\mathrm{i}k\bar{x}} \, \mathrm{d}\bar{x}.$$

In the following, $(\widehat{u}, \widehat{v}, \widehat{p}, \widehat{\rho})$ will stand for the Fourier transform of $(\tilde{u}, \tilde{v}, \tilde{p}, \tilde{\rho})$. Throughout § 3.1–§ 3.3, expansions in each deck will be given for $(\widehat{u}, \widehat{v}, \widehat{p}, \widehat{\rho})$. The inversion contour in the k-plane will be chosen to ensure that the solution is causal.

3. Triple-deck solution

In this section, we consider the solutions in each of the three decks. These solutions must be obtained up to $O(\epsilon^2)$ accuracy even for the purpose of determining the leading-order acoustic radiation in the far field. The reason is that the near-field solutions at the first three consecutive orders are such that they represent the quadrupole, dipole and monopole respectively, which turn out to make an equal order-of-magnitude contribution to the far field acoustic radiation.

3.1. *The main deck*

In the main deck, it is convenient to use renormalized variable

$$\tilde{y} = (T_w/T_\infty)^{-1} y.$$

The Fourier transform of the unsteady flow has the expansion

$$\widehat{u} = \epsilon (T_w/T_\infty)^{1/2} [U_1 + \epsilon U_2 + \epsilon^2 U_3 + \cdots], \tag{3.1}$$

$$\widehat{v} = \epsilon^2 [V_1 + \epsilon V_2 + \epsilon^2 V_3 + \cdots], \tag{3.2}$$

$$\widehat{\rho} = \epsilon (T_w/T_\infty)^{1/2} [R_1 + \epsilon R_2 + \epsilon^2 R_3 + \cdots], \tag{3.3}$$

$$\widehat{p} = \epsilon^2 [P_1 + \epsilon P_2 + \epsilon^2 P_3 + \cdots]. \tag{3.4}$$

For the purpose of calculating the sound, there is no need to go beyond the present three-term expansion, and the reason for this will be given at the end of § 5.1.

The leading-order terms satisfy the familiar main-deck equations, and have the well-known solution (e.g. Stewartson 1974)

$$U_1 = A_1 U_B', \quad V_1 = -\mathrm{i}k A_1 U_B, \quad R_1 = A_1 R_B', \tag{3.5}$$

where A_1 is a function of k to be determined by matching, and the prime denotes the derivative with respect to $\tilde{y}$.

The $O(R^{-1/8})$ correction terms, U_2, V_2 etc., are governed by

$$\mathrm{i}k(R_B U_2 + U_B R_2) + \frac{\partial}{\partial \tilde{y}}(R_B V_2) = \mathrm{i}\omega R_1, \tag{3.6}$$

$$R_B(\mathrm{i}k U_B U_2 + U_B' V_2) = \mathrm{i}\omega R_B U_1 - \Omega \mathrm{i}k P_1, \tag{3.7}$$

$$\mathrm{i}k U_B R_2 + R_B' V_2 = \mathrm{i}\omega R_1 + \Omega \mathrm{i}k P_1 M^2 R_B U_B, \tag{3.8}$$

$$\mathrm{i}k \Omega R_B U_B V_1 = -P_{2,\tilde{y}}, \tag{3.9}$$

where $\Omega = (T_w/T_\infty)^{-1/2}$. On eliminating U_2 and R_2 among (3.6)–(3.8), it can be shown

that

$$R_B(U_B V_2' - U_B' V_2) = \Omega \mathrm{i}kP_1(1 - M^2 R_B U_B^2) - \mathrm{i}\omega A_1 R_B U_B'. \tag{3.10}$$

After inserting in (3.5), equation (3.10) is solved to give

$$V_2 = -\mathrm{i}kA_2 U_B + \mathrm{i}\omega A_1 + \Omega \mathrm{i}kP_1 U_B \int^{\tilde{y}} \left(\frac{1}{R_B U_B^2} - M^2 \right) \mathrm{d}\tilde{y}, \tag{3.11}$$

while (3.9) gives

$$P_2 = \tilde{P}_2 - k^2 A_1(k) \Omega \int_0^{\tilde{y}} R_B U_B^2 \, \mathrm{d}\tilde{y}, \tag{3.12}$$

where A_2 and $\tilde{P}_2$ are functions of k to be found later. It is easy to show that as $\tilde{y} \to \infty$

$$\left.\begin{aligned} V_2 &\to \Omega(\mathrm{i}kP_1)(1 - M^2)\tilde{y} + (-\mathrm{i}kA_2 + \mathrm{i}\omega A_1 + \Omega \mathrm{i}kP_1 J_\infty) + \cdots, \\ P_2 &\to (-\Omega k^2 A_1)\tilde{y} + (\tilde{P}_2 - \Omega k^2 A_1 I_2) + \cdots, \end{aligned}\right\} \tag{3.13}$$

where J_∞ and I_2 are defined respectively by (A 4) and (A 2) in the Appendix. On the other hand, as $\tilde{y} \to 0$,

$$V_2 \to \mathrm{i}\omega A_1 - \Omega(T_w/T_\infty)\lambda^{-1}\mathrm{i}kP_1 + (-\mathrm{i}k\lambda A_2 + \Omega \mathrm{i}kP_1 \lambda J_0)\, \tilde{y} + \cdots,$$

with J_0 being given by (A 3).

The governing equations for U_3 and V_3 are

$$\mathrm{i}k(R_B U_3 + U_B R_3) + \frac{\partial}{\partial \tilde{y}}(R_B V_3) = \mathrm{i}\omega R_2, \tag{3.14}$$

$$R_B(\mathrm{i}kU_B U_3 + U_B' V_3) = \mathrm{i}\omega R_B U_2 - \Omega \mathrm{i}kP_2, \tag{3.15}$$

$$\mathrm{i}kU_B R_3 + R_B' V_3 = \mathrm{i}\omega R_2 + \Omega M^2 R_B(\mathrm{i}kP_2 U_B - \mathrm{i}\omega P_1), \tag{3.16}$$

$$\Omega R_B(-\mathrm{i}\omega V_1 + \mathrm{i}kU_B V_2) = -P_{3,\tilde{y}}. \tag{3.17}$$

These equations can be solved to give

$$\begin{aligned} V_3 = {} & -\mathrm{i}kA_3 U_B + \mathrm{i}\omega A_2 + \Omega(\mathrm{i}k\tilde{P}_2)U_B \int^{\tilde{y}} \left(\frac{1}{R_B U_B^2} - M^2 \right) \mathrm{d}\tilde{y} \\ & - \Omega^2(\mathrm{i}k^3)A_1 U_B \int_0^{\tilde{y}} \left(\frac{1}{R_B U_B^2} - M^2 \right) \int_0^{\tilde{y}_2} R_B U_B^2 \, \mathrm{d}\tilde{y}_1 \, \mathrm{d}\tilde{y}_2 \\ & + \Omega(\mathrm{i}\omega P_1)U_B \left\{ 2 \int^{\tilde{y}} \frac{1}{R_B U_B^3} \, \mathrm{d}\tilde{y} - \frac{1}{U_B} \int^{\tilde{y}} \left(\frac{1}{R_B U_B^2} - M^2 \right) \mathrm{d}\tilde{y} \right\}, \end{aligned} \tag{3.18}$$

$$\begin{aligned} P_3 = \tilde{P}_3 + \Omega \Big\{ & 2\omega k A_1 \int_0^{\tilde{y}} R_B U_B \mathrm{d}\tilde{y} - k^2 A_2 \int_0^{\tilde{y}} R_B U_B^2 \, \mathrm{d}\tilde{y} \\ & + \Omega k^2 P_1 \int_0^{\tilde{y}} R_B U_B^2 \int^{\tilde{y}_2} \left(\frac{1}{R_B U_B^2} - M^2 \right) \mathrm{d}\tilde{y}_1 \mathrm{d}\tilde{y}_2 \Big\}, \end{aligned} \tag{3.19}$$

where A_3 and $\tilde{P}_3$ are functions of k to be determined. It can be shown that as $\tilde{y} \to \infty$

$$\begin{aligned} V_3 \to {} & -\tfrac{1}{2}(1 - M^2)\Omega^2 \mathrm{i}k^3 A_1 \tilde{y}^2 + \{-\Omega^2 \mathrm{i}k^3(1 - M^2)I_2 A_1 + \Omega \mathrm{i}\omega(1 + M^2)P_1\}\tilde{y} \\ & + \{\Omega \mathrm{i}k\tilde{P}_2 J_\infty + \Omega \mathrm{i}\omega P_1 H_6^\infty - \Omega^2 \mathrm{i}k^3 A_1 H_5 - \mathrm{i}kA_3 + \mathrm{i}\omega A_2\} + \cdots, \end{aligned} \tag{3.20}$$

$$P_3 \to \tfrac{1}{2}(1-M^2)\Omega^2 k^2 P_1 \tilde{y}^2 + \Omega\{2\omega k A_1 - k^2 A_2 + \Omega k^2 P_1 J_\infty\}\tilde{y}$$
$$+\Omega\{2\omega k A_1 I_1 - k^2 A_2 I_2 + \Omega k^2 P_1 H_3\} + \cdots, \tag{3.21}$$

where H_6^∞, H_5, I_1 and H_3 are defined by (A 7), (A 6), (A 1) and (A 5) respectively. Elimination of R_3 between equations (3.14) and (3.16) yields

$$\mathrm{i}kU_3 + V_3' = -\Omega M^2 \mathrm{i}k P_2 U_B + \Omega M^2 \mathrm{i}\omega P_1,$$

using which, together with (3.18), we find that as $\tilde{y} \to 0$

$$U_3 \sim 2\Omega(\gamma-1)M^2 \frac{\omega P_1}{k} \ln \tilde{y} + \lambda A_3 + \Omega \left\{ -\lambda J_0 \tilde{P}_2 - \frac{\omega\lambda}{k} H_6^{(0)} P_1 \right\}, \tag{3.22}$$

with $H_6^{(0)}$ being given by (A 8).

3.2. *The upper-deck solution*

In the upper deck, the transverse variable $\bar{y}$ is defined as

$$\bar{y} = K^{-1}(\epsilon y) = (T_w/T_\infty)^{-1/2}(\epsilon\tilde{y}), \tag{3.23}$$

and the Fourier transform of the solution for the unsteady flow expands as

$$\hat{v} = \epsilon^2(\bar{v}_1 + \epsilon\bar{v}_2 + \epsilon^2\bar{v}_3 + \cdots), \tag{3.24}$$

$$\hat{p} = \epsilon^2(\bar{p}_1 + \epsilon\bar{p}_2 + \epsilon^2\bar{p}_3 + \cdots). \tag{3.25}$$

The governing equations for $\bar{p}_1$ and $\bar{v}_1$ are

$$\left\{ \frac{\partial^2}{\partial\bar{y}^2} - (1-M^2)k^2 \right\} \bar{p}_1 = 0, \quad \mathrm{i}k\bar{v}_1 = -\bar{p}_{1,\bar{y}},$$

which have the solution

$$\bar{p}_1 = P_1 \mathrm{e}^{-\bar{\kappa}\bar{y}}, \quad \bar{v}_1 = \frac{\bar{\kappa}}{\mathrm{i}k} P_1 \mathrm{e}^{-\bar{\kappa}\bar{y}}, \tag{3.26}$$

where

$$\bar{\kappa} = (1-M^2)^{1/2}[(k+\mathrm{i}0)(k-\mathrm{i}0)]^{1/2}; \tag{3.27}$$

here $(k \pm \mathrm{i}0)$ indicates that a small positive/negative quantity has been added to k, and the branch cuts of $(k \pm \mathrm{i}0)^{1/2}$ are taken to be in the lower/upper half-planes. Matching $\bar{v}_1$ with the main-deck solution V_1 in (3.5) gives

$$P_1 = k^2/\bar{\kappa}A_1. \tag{3.28}$$

The governing equations for $\bar{p}_2$ and $\bar{v}_2$ in (3.24)–(3.25) are

$$\left\{ \frac{\partial^2}{\partial\bar{y}^2} - (1-M^2)k^2 \right\} \bar{p}_2 = 2M^2\omega k\bar{p}_1, \quad \mathrm{i}k\bar{v}_2 - \mathrm{i}\omega\bar{v}_1 = -\bar{p}_{2,\bar{y}}.$$

The solution for $\bar{p}_2$ is

$$\bar{p}_2 = \bar{P}_2 \mathrm{e}^{-\bar{\kappa}\bar{y}} - \frac{M^2\omega k}{\bar{\kappa}} P_1 \bar{y} \mathrm{e}^{-\bar{\kappa}\bar{y}}, \tag{3.29}$$

where $\bar{P}_2$ is an arbitrary function of k. It follows from substituting $\bar{p}_2$ into the equation for $\bar{v}_2$, that as $\bar{y} \to 0$

$$\bar{v}_2 \to \frac{\bar{\kappa}}{\mathrm{i}k}\bar{P}_2 - \frac{\mathrm{i}\omega}{\bar{\kappa}} P_1.$$

The matching requirements for the pressure and vertical velocity with their main-deck counterparts lead to

$$\bar{P}_2 = \tilde{P}_2 - \Omega k^2 A_1 I_2, \tag{3.30}$$

$$\frac{\bar{\kappa}}{\mathrm{i}k}\bar{P}_2 - \frac{\mathrm{i}\omega}{\bar{\kappa}}P_1 = -\mathrm{i}kA_2 + \mathrm{i}\omega A_1 + \Omega(\mathrm{i}kP_1)J_\infty. \tag{3.31}$$

The functions $\bar{p}_3$ and $\bar{v}_3$ satisfy

$$\left\{\frac{\partial^2}{\partial \bar{y}^2} - (1-M^2)k^2\right\}\bar{p}_3 = 2M^2\omega k\bar{p}_2 - M^2\omega^2\bar{p}_1, \quad \mathrm{i}k\bar{v}_3 - \mathrm{i}\omega\bar{v}_2 = -\bar{p}_{3,\bar{y}}. \tag{3.32}$$

The solution for $\bar{p}_3$ is found to be

$$\bar{p}_3 = \bar{P}_3\,\mathrm{e}^{-\bar{\kappa}\bar{y}} + \frac{M^4\omega^2}{2(1-M^2)}P_1\bar{y}^2\,\mathrm{e}^{-\bar{\kappa}\bar{y}} + \left\{\frac{M^2\omega^2 P_1}{2(1-M^2)\bar{\kappa}} - \frac{M^2\omega k\bar{P}_2}{\bar{\kappa}}\right\}\bar{y}\,\mathrm{e}^{-\bar{\kappa}\bar{y}}. \tag{3.33}$$

It follows from (3.32) that as $\bar{y} \to 0$

$$\bar{v}_3 \to \frac{\bar{\kappa}}{\mathrm{i}k}\bar{P}_3 - \frac{\mathrm{i}\omega}{\bar{\kappa}}\bar{P}_2 - \frac{\mathrm{i}\omega^2 P_1}{\bar{\kappa}k}\left[1 - \frac{M^2}{2(1-M^2)}\right].$$

Matching the pressure $\bar{p}_3$ and the vertical velocity $\bar{v}_3$ with their respective counterparts in the main deck yields

$$\bar{P}_3 = \tilde{P}_3 + \Omega\{2\omega k A_1 I_1 - k^2 A_2 I_2 + \Omega k^2 P_1 H_3\}, \tag{3.34}$$

$$\frac{\bar{\kappa}}{\mathrm{i}k}\bar{P}_3 - \frac{\mathrm{i}\omega}{\bar{\kappa}}\bar{P}_2 - \frac{\mathrm{i}\omega^2 P_1}{\bar{\kappa}k}\left[1 - \frac{M^2}{2(1-M^2)}\right] = \Omega\mathrm{i}k\tilde{P}_2 J_\infty + \Omega\mathrm{i}\omega P_1 H_6^\infty - \Omega^2\mathrm{i}k^3 A_1 H_5 - \mathrm{i}kA_3 + \mathrm{i}\omega A_2. \tag{3.35}$$

3.3. *The lower-deck solution*

The local transverse variable for the lower deck is

$$Y = \epsilon^{-1}(T_w/T_\infty)^{-3/2}y = \epsilon^{-1}(T_w/T_\infty)^{-1/2}\tilde{y},$$

and the Fourier transform of the unsteady field has the expansion

$$\hat{u} = \epsilon(T_w/T_\infty)^{1/2}\left[\tilde{U}_1 + \epsilon\tilde{U}_2 + \epsilon^2\tilde{U}_3 + \cdots\right], \tag{3.36}$$

$$\hat{v} = \epsilon^3(T_w/T_\infty)^{1/2}\left[\tilde{V}_1 + \epsilon\tilde{V}_2 + \epsilon^2\tilde{V}_3 + \cdots\right], \tag{3.37}$$

$$\hat{p} = \epsilon^2\left[P_1 + \epsilon\tilde{P}_2 + \epsilon^2\tilde{P}_3 + \cdots\right], \tag{3.38}$$

$$\hat{\rho} = \epsilon^2(T_w/T_\infty)^{-1}\left[R_1 + \epsilon R_2 + \epsilon^2 R_3 + \cdots\right]. \tag{3.39}$$

The leading-order terms satisfy the linearized boundary-layer equations

$$\mathrm{i}k\tilde{U}_1 + \tilde{V}_{1,Y} = 0, \tag{3.40}$$

$$\mathrm{i}(k\lambda Y - \hat{\omega})\tilde{U}_1 + \lambda\tilde{V}_1 = -\mathrm{i}kP_1 + \tilde{U}_{1,YY}, \tag{3.41}$$

where $\hat{\omega} = \omega(T_w/T_\infty)^{-1/2}$. The above system is subject to the matching condition with the main deck:

$$\tilde{U}_1 \to \lambda A_1 \quad \text{as} \quad Y \to \infty, \tag{3.42}$$

and the boundary condition on the wall: $\tilde{U}_1 = 0$, $\tilde{V}_1 = \widehat{V}_s$ at $Y = 0$. The latter implies that

$$\tilde{U}_{1,YY}(0) = \lambda \widehat{V}_s + \mathrm{i}kP_1 \tag{3.43}$$

after setting $Y = 0$ in (3.41). By eliminating the pressure from (3.40)–(3.41), it can be shown that $\tilde{U}_1$ satisfies

$$\left\{ \frac{\partial^2}{\partial Y^2} - \mathrm{i}(k\lambda Y - \hat{\omega}) \right\} \tilde{U}_{1,Y} = 0. \tag{3.44}$$

The solution is

$$\tilde{U}_1 = C_1(k) \int_{\zeta_0}^{\zeta} \mathrm{Ai}(\zeta)\, \mathrm{d}\zeta, \tag{3.45}$$

where $C_1(k)$ is to be found, Ai denotes the Airy function, and

$$\zeta = (\mathrm{i}k\lambda)^{1/3} Y + \zeta_0, \quad \zeta_0 = -\mathrm{i}\hat{\omega}(\mathrm{i}k\lambda)^{-2/3}. \tag{3.46}$$

Application of (3.42) and (3.43) together with (3.46) gives

$$C_1(k) \int_{\zeta_0}^{\infty} \mathrm{Ai}(\zeta)\, \mathrm{d}\zeta = \lambda A_1, \tag{3.47}$$

$$(\mathrm{i}k\lambda)^{2/3} C_1(k) \mathrm{Ai}'(\zeta_0) = \lambda \widehat{V}_s + \mathrm{i}kP_1. \tag{3.48}$$

Eliminating A_1 and $C_1(k)$ from (3.28), (3.47) and (3.48), we obtain

$$P_1 = \frac{\mathrm{i}\lambda \widehat{V}_s(k)}{k\Delta(k)} \int_{\zeta_0}^{\infty} \mathrm{Ai}(\zeta)\, \mathrm{d}\zeta, \tag{3.49}$$

where

$$\Delta(k) = \int_{\zeta_0}^{\infty} \mathrm{Ai}(\zeta)\, \mathrm{d}\zeta + \mathrm{i}\lambda(\mathrm{i}k\lambda)^{2/3} \mathrm{Ai}'(\zeta_0) \frac{\bar{\kappa}}{k^3}. \tag{3.50}$$

Consider now the terms $\tilde{U}_2$ and $\tilde{V}_2$ in the expansion (3.36)–(3.38). They are governed by the same equations as $\tilde{U}_1$ and $\tilde{V}_1$, but satisfy the boundary conditions at the wall, $\tilde{U}_2 = \tilde{V}_2 = 0$ at $Y = 0$, which are equivalent to

$$\tilde{U}_2 = 0, \quad \tilde{U}_{2,YY} = \mathrm{i}k\tilde{P}_2 \quad \text{at} \quad Y = 0. \tag{3.51}$$

The solution satisfying the first of the above conditions is

$$\tilde{U}_2 = C_2(k) \int_{\zeta_0}^{\zeta} \mathrm{Ai}(\zeta)\, \mathrm{d}\zeta, \tag{3.52}$$

where $C_2(k)$ is a function of k. Application of the second condition in (3.51) gives

$$(\mathrm{i}k\lambda)^{2/3} C_2 \mathrm{Ai}'(\zeta_0) = \mathrm{i}k\tilde{P}_2, \tag{3.53}$$

while matching $\tilde{U}_2$ with its counterpart in the main deck leads to

$$C_2 \int_{\zeta_0}^{\infty} \mathrm{Ai}(\zeta)\, \mathrm{d}\zeta = -\Omega P_1 \lambda J_0 + \lambda A_2. \tag{3.54}$$

After eliminating A_2 and $\tilde{P}_2$ from (3.30)–(3.31) and (3.53)–(3.54), we find that

$$\bar{P}_2 = -\frac{(\mathrm{i}k\lambda)^{2/3} \lambda \mathrm{Ai}'(\zeta_0)}{k^2 \Delta(k)} \left\{ \frac{\omega(2 - M^2)}{k\bar{\kappa}} + \Omega \left[J_\infty - J_0 - (1 - M^2) I_2 \right] \right\} (\mathrm{i}kP_1) - \Omega I_2 \bar{\kappa} P_1. \tag{3.55}$$

The terms $\tilde{U}_3$, $\tilde{V}_3$ etc., in (3.36)–(3.38) are governed by the equations

$$\mathrm{i}k\tilde{U}_3 + \tilde{V}_{3,Y} = -\Omega_3 Y \tilde{V}_1 + (\mathrm{i}\hat{\omega} - \mathrm{i}k\lambda Y)R_1, \tag{3.56}$$

$$\mathrm{i}(k\lambda Y - \hat{\omega})\tilde{U}_3 + \lambda\tilde{V}_3 = -\mathrm{i}k\tilde{P}_3 + \tilde{U}_{3,YY} + \tfrac{1}{2}\Omega_3(Y^2(\mathrm{i}kP_1) - 2Y^2\tilde{U}_{1,YY} - 2Y\tilde{U}_{1,Y})$$
$$-\Omega_3(\tfrac{1}{6}\lambda Y^3\mathrm{i}k\tilde{U}_1 + \tfrac{1}{2}\lambda Y^2\tilde{V}_1) - \lambda R_{1,Y}, \tag{3.57}$$

$$R_{1,YY} + \mathrm{i}(\hat{\omega} - k\lambda Y)R_1 = \Omega_3\lambda^{-1}(\lambda Y\tilde{V}_1 + 2\tilde{U}_{1,Y}) + M^2(\mathrm{i}\hat{\omega} - \mathrm{i}k\lambda Y)P_1, \tag{3.58}$$

where $\Omega_3 = (\gamma - 1)M^2\lambda^2$. After eliminating $\tilde{P}_3$ from (3.56)–(3.58), we find

$$\left\{\frac{\partial^2}{\partial Y^2} - \mathrm{i}(k\lambda Y - \hat{\omega})\right\}\tilde{U}_{3,Y}$$
$$= \Omega_3\{Y(\mathrm{i}\hat{\omega} - \mathrm{i}k\lambda Y)\tilde{U}_1 + 2Y(-\mathrm{i}kP_1) + Y^2\tilde{U}_{1,YYY} + 4Y\tilde{U}_{1,YY} + 3\tilde{U}_{1,Y}$$
$$+\tfrac{1}{6}Y^3(\mathrm{i}k\lambda)\tilde{U}_{1,Y}\} + M^2\lambda(\mathrm{i}\hat{\omega} - \mathrm{i}k\lambda Y)P_1. \tag{3.59}$$

In order to express the solution in a form that is convenient for evaluating its large-Y asymptote, we write

$$\tilde{U}_3 = \left(2\lambda^{-1}\Omega_3 + M^2\lambda\right)P_1 Y + \Omega_3\int_0^Y Y\tilde{U}_1\,\mathrm{d}Y + \Omega_3\tilde{W}_3. \tag{3.60}$$

Then $\tilde{W}_3$ satisfies

$$\tilde{W}_{3,\zeta\zeta\zeta} - \zeta\tilde{W}_{3,\zeta} = (\mathrm{i}k\lambda)^{-2/3}\{\tfrac{1}{6}(\zeta - \zeta_0)^3\tilde{U}_{1,\zeta} + (\zeta - \zeta_0)^2\tilde{U}_{1,\zeta\zeta\zeta} + 3(\zeta - \zeta_0)\tilde{U}_{1,\zeta\zeta} + \tilde{U}_{1,\zeta}\}$$
$$-2\lambda^{-1}(\mathrm{i}k\lambda)^{-1}(\mathrm{i}\hat{\omega})P_1. \tag{3.61}$$

We find that

$$\tilde{W}_{3,\zeta} = (\mathrm{i}k\lambda)^{-2/3}\{\tfrac{1}{6}(\zeta - \zeta_0)^3\tilde{U}_{1,\zeta\zeta} + (\tfrac{1}{2}\zeta^2 - \zeta_0\zeta)\tilde{U}_{1,\zeta}\} + C_3(k)\mathrm{Ai}(\zeta) - \frac{2\hat{\omega}}{\lambda^2 k}P_1 M(\zeta, \zeta_0), \tag{3.62}$$

where C_3 is a function of k, and

$$M(\zeta, \zeta_0) = \pi\left\{\mathrm{Bi}(\zeta)\int_\infty^\zeta \mathrm{Ai}(\zeta)\,\mathrm{d}\zeta - \mathrm{Ai}(\zeta)\int_{\zeta_0}^\zeta \mathrm{Ai}(\zeta)\,\mathrm{d}\zeta\right\},$$

with Bi being the second Airy function. Integrating (3.62) once and inserting it into (3.60) gives $\tilde{U}_3$. Matching $\tilde{U}_3$ with the main-deck solution (3.22), we obtain

$$-\Omega\left\{\lambda J_0\tilde{P}_2 + \frac{\omega\lambda}{k}H_6^{(0)}P_1\right\} + \lambda A_3 = -(\mathrm{i}k\lambda)^{-2/3}\Omega_3\Lambda_\infty + C_3(k)\int_{\zeta_0}^\zeta \mathrm{Ai}(\zeta)\,\mathrm{d}\zeta, \tag{3.63}$$

where

$$\Lambda_\infty = \zeta_0^2\lambda A_1 + \tfrac{1}{2}\{\zeta_0\tilde{U}_{1,\zeta\zeta}(\zeta_0) + \tilde{U}_{1,\zeta}(\zeta_0)\}$$
$$+2\lambda^{-1}\zeta_0(\mathrm{i}k\lambda)^{1/3}P_1\left\{\int_{\zeta_0}^\infty\left\{M(\zeta, \zeta_0) + \frac{1}{\zeta}\right\}\mathrm{d}\zeta + \ln\left((T_w/T_\infty)^{1/2}\zeta_0(\mathrm{i}k\lambda)^{1/3}\right)\right\}.$$

The boundary condition at the wall yields

$$-\Omega_3\Lambda_0 + (\mathrm{i}k\lambda)^{2/3}C_3(k)\mathrm{Ai}'(\zeta_0) = \mathrm{i}k\tilde{P}_3, \tag{3.64}$$

with

$$\Lambda_0 = \tfrac{1}{2}\zeta_0^2\tilde{U}_{1,\zeta\zeta}(\zeta_0) + 2\pi\lambda^{-1}\zeta_0(\mathrm{i}k\lambda)^{1/3}P_1\mathrm{Bi}(\zeta_0)\int_{\zeta_0}^{\infty}\mathrm{Ai}(\zeta)\,\mathrm{d}\zeta.$$

The solution for $\bar{P}_3$ can be found from (3.34)–(3.35), (3.63) and (3.64),

$$\begin{aligned}\bar{P}_3 = &-\frac{\mathrm{i}\mathrm{Ai}'(\zeta_0)}{k\Delta(k)}\Omega_3\left\{\Lambda_\infty - \Lambda_0\int_{\zeta_0}^{\infty}\mathrm{Ai}(\zeta)\,\mathrm{d}\zeta/\mathrm{Ai}'(\zeta_0)\right\}\\ &+\frac{(\mathrm{i}k\lambda)^{2/3}\lambda\mathrm{Ai}'(\zeta_0)}{k^2\Delta(k)}\left\{-\frac{\mathrm{i}\omega\bar{P}_2}{\bar{\kappa}} - \frac{\mathrm{i}\omega^2P_1}{k\bar{\kappa}}\left[1-\frac{M^2}{2(1-M^2)}\right] - \mathrm{i}\omega A_2 - \Omega\chi\right\}\\ &+\Omega\left\{2\omega k A_1 I_1 - k^2A_2I_2 + \Omega k^2P_1H_3\right\},\end{aligned} \tag{3.65}$$

where

$$\begin{aligned}\chi = &\,k\bar{\kappa}A_2I_2 - k(\bar{P}_2 + \Omega I_2\bar{\kappa}P_1)(J_\infty - J_0)\\ &-\omega\left[H_6^\infty - H_6^0 + 2(1-M^2)I_1\right]P_1 + \Omega k\bar{\kappa}P_1(H_5 - H_3).\end{aligned}$$

4. Receptivity: the amplitude of T–S waves

The results in the previous section allow us to calculate the amplitude of the T–S wave. The leading-order solution has already been given by Terent'ev (1981, 1984). We now show how the T–S wave can be determined up to $O(\epsilon)$ accuracy.

To be specific, we consider the solution in the lower deck. The first two terms of its Fourier transform are given by (3.45) and (3.52). Thus the solution in the physical space, accurate up to $O(\epsilon)$, is given by

$$\tilde{u} = \frac{1}{(2\pi)^{1/2}}\int_{-\infty}^{\infty}\left\{[C_1(k) + \epsilon C_2(k)]\int_{\zeta_0}^{\zeta}\mathrm{Ai}(\zeta)\,\mathrm{d}\zeta\right\}\mathrm{e}^{\mathrm{i}(k\bar{x}-\omega\bar{t})}\,\mathrm{d}k + O(\epsilon^2). \tag{4.1}$$

Here the function $C_1(k)$ is found from (3.28), (3.47) and (3.48),

$$C_1(k) = \frac{\mathrm{i}\lambda^2\widehat{V}_s(k)\bar{\kappa}}{k^3\Delta(k)}, \tag{4.2}$$

while $C_2(k)$ is solved from (3.30)–(3.31) and (3.53)–(3.54),

$$C_2(k) = \frac{\mathrm{i}\lambda^2\widehat{V}_s(k)}{k\Delta^2(k)}\left\{\frac{(2-M^2)\omega}{k\bar{\kappa}} + \Omega\left(J_\infty - J_0 - (1-M^2)I_2\right)\right\}\int_{\zeta_0}^{\infty}\mathrm{Ai}(\zeta)\,\mathrm{d}\zeta. \tag{4.3}$$

The above expressions show that $C_1(k)$ and $C_2(k)$ have simple and double poles respectively at $k = \alpha$ where α is any root of Δ, i.e.

$$\Delta(\alpha) = 0. \tag{4.4}$$

This equation is the leading-order dispersion relation of the T–S waves. It is known that for a given real frequency $\hat{\omega}$, at most one root lies in the lower half-plane. The integration contour that ensures the causality depends on the location of the roots. If all the roots lie in the upper half-plane, the integration contour (4.1) can be taken to be along the real axis. But if one of the roots is in the lower half-plane the contour has to be deformed to lie below that root. In either case, the T–S wave corresponds to $2\pi\mathrm{i}$ times the residue of the integrand in (4.1) at $k = \alpha$. We find that

$$\tilde{u}_{TS} = -(2\pi)^{\frac{1}{2}}\frac{\lambda^2\widehat{V}_s(\alpha)(1-M^2)^{1/2}}{\alpha^2\Delta'(\alpha)}\left\{\tilde{U}_{TS} + \epsilon(\mathrm{i}\alpha\bar{x})q_c\int_{\zeta_0}^{\zeta}\mathrm{Ai}(\zeta)\,\mathrm{d}\zeta\right\}\mathrm{e}^{\mathrm{i}(\alpha\bar{x}-\omega\bar{t})}, \tag{4.5}$$

where

$$\tilde{U}_{TS} = (1+\epsilon q_\infty)\int_{\zeta_0}^{\zeta} \mathrm{Ai}(\zeta)\,\mathrm{d}\zeta + \epsilon \tfrac{1}{3} q_c\,[(\zeta - 3\zeta_0)\mathrm{Ai}(\zeta) + 2\zeta_0 \mathrm{Ai}(\zeta_0)]\,, \tag{4.6}$$

$$q_\infty = \frac{1}{(1-M^2)^{1/2}\Delta'(\alpha)}\left\{\left\{\left(\frac{\alpha \widehat{V}_s'(\alpha)}{\widehat{V}_s(\alpha)} - 1 - \frac{\alpha\Delta''(\alpha)}{\Delta'(\alpha)}\right)\Lambda - \frac{2(2-M^2)\omega}{(1-M^2)^{1/2}\alpha^2}\right\} \times \int_{\zeta_0}^{\infty} \mathrm{Ai}(\zeta)\,\mathrm{d}\zeta + \tfrac{2}{3}\Lambda\zeta_0 \mathrm{Ai}(\zeta_0)\right\}, \tag{4.7}$$

$$q_c = \frac{\Lambda}{(1-M^2)^{1/2}\Delta'(\alpha)}\int_{\zeta_0}^{\infty} \mathrm{Ai}(\zeta)\,\mathrm{d}\zeta, \tag{4.8}$$

with

$$\Lambda = \frac{(2-M^2)\omega}{(1-M^2)^{1/2}\alpha^2} + \Omega\left(J_\infty - J_0 - (1-M^2)I_2\right). \tag{4.9}$$

Due to its exponential growth, the T–S wave will eventually dominate the flow further downstream. However, the presence of the secular term proportional to $\bar{x}$ in (4.5) implies that (4.5) is no longer valid when $\bar{x} = O(R^{1/8})$. In order to interpret this term properly and also to be precise about what the theory can predict, we must consider the subsequent development of the T–S wave. In the second phase where $\bar{x} \gg R^{1/8}$ or equivalently $x \gg R^{-1/4}$, the T–S wave is governed by local parallel stability theory, and its solution, the streamwise velocity in the lower deck say, takes the usual WKBJ form

$$u_{TS} = A_I U_{TS}(Y, x; \epsilon)\exp\left\{\mathrm{i}R^{3/8}\int_0^x \alpha_{TS}(x)\,\mathrm{d}x - \mathrm{i}\omega\bar{t}\right\}, \tag{4.10}$$

where the constant A_I is the (unknown) amplitude of the T–S wave, and U_{TS} is the eigenfunction. The complex wavenumber $\alpha_{TS}(x)$ has the expansion

$$\alpha_{TS} = \alpha_1(x) + \epsilon\alpha_2(x) + \cdots,$$

with α_1, α_2 etc., being determined by an analysis very similar to that in § 3. The leading-order analysis immediately shows that α_1 is a root of $\Delta(\alpha_1) = 0$, with of course λ now standing for the local wall shear, i.e. $\lambda = 0.332(1+x)^{-1/2}$. After carrying on the analysis to the second order, we find that

$$\alpha_2 = \frac{\alpha_1^2}{(1-M^2)^{1/2}a}\left\{\frac{(2-M^2)\omega}{(1-M^2)^{1/2}\alpha_1^2} + \Omega(J_\infty - J_0 - (1-M^2)I_2)\right\}\int_{\zeta_0}^{\infty} \mathrm{Ai}(\zeta)\,\mathrm{d}\zeta, \tag{4.11}$$

where the constant a is defined by

$$a = \tfrac{2}{3}\zeta_0 \mathrm{Ai}(\zeta_0) + 2\int_{\zeta_0}^{\infty} \mathrm{Ai}(\zeta)\,\mathrm{d}\zeta + \tfrac{2}{3}(1-M^2)^{1/2}\frac{(\mathrm{i}\alpha_1\lambda)^{5/3}}{\alpha_1^3}\{\mathrm{Ai}'(\zeta_0) - \zeta_0^2\mathrm{Ai}(\zeta_0)\}. \tag{4.12}$$

Obviously the dependence of α_1 and α_2 on the slow variable x is parametric. It follows that as $x \to 0$, $\alpha_1 \to \alpha$, and

$$u_{TS} \approx A_I U_{TS}(Y, 0; \epsilon)\,(1 + \epsilon\mathrm{i}\alpha_2\bar{x})\,\mathrm{e}^{\mathrm{i}(\alpha\bar{x} - \omega\bar{t})}. \tag{4.13}$$

Matching the leading-order terms in (4.5) and (4.10) gives

$$u_I \equiv A_I U_{TS}(Y, 0; \epsilon) = -(2\pi)^{1/2}\frac{\lambda^2 \widehat{V}_s(\alpha)(1-M^2)^{1/2}}{\alpha^2\Delta'(\alpha)}\tilde{U}_{TS}. \tag{4.14}$$

It is easy to verify that $a = \alpha\Delta'(\alpha)$, and then (4.8) and (4.11) show that $\alpha_2 = \alpha q_c$. Therefore to the required order, the terms proportional to $\bar{x}$ in (4.5) and (4.13) match automatically. It now transpires that the secular term in (4.5) is associated with the second-order correction to the dispersion relation of the T–S wave, while $\tilde{U}_{TS}$ given by (4.6) is the T–S eigenfunction, accurate up to $O(\epsilon)$.

In experiments on localized receptivity such as the case studied here, one usually has to measure the streamwise velocity of the T–S wave at some distance downstream, where the wave has attained a sizeable magnitude. That velocity is then extrapolated back to give the velocity at the location of forcing. As (4.10) indicates, the u_I given by (4.14) represents exactly this extrapolated velocity. It is worth noting that although u_I is often referred to as the initial streamwise velocity of the T–S wave, it is *not* the physical velocity measured directly at the position of suction; the latter is far more complex.

Equation (4.14) along with (4.6)–(4.9) determines the initial amplitude of the T–S wave to $O(\epsilon)$ accuracy. These results represent an extension of the earlier result of Terent'ev (1981, 1984). It would be straightforward to work out the T–S wave amplitude to $O(\epsilon^2)$, though a much more complex calculation is required. The procedure given in this section has been applied, with some modifications, to construct a second-order theory for the localized receptivity involving a vortical free-stream disturbance interacting with a local roughness (Wu 2001*b*), where a quantitative comparison was made with the experimental data of Dietz (1999). For the distributed receptivity, a second-order theory was completed by the author (Wu 2001*a*). In both cases, good agreement with experiments was obtained.

The Blasius profile and the Airy function $\mathrm{Ai}(\eta)$ are obtained by a shooting method based on a fourth-order Runge–Kutta method. The various integrals are evaluated using the Trapezoidal rule or Simpson's rule wherever possible. The calculations are performed for uniform suction, i.e.

$$V_s(\bar{x}) = \begin{cases} V_0 & \text{when} \quad |\bar{x}| \leqslant D, \\ 0 & \text{otherwise.} \end{cases} \tag{4.15}$$

We define the coupling coefficient

$$C_p = u_I / D V_0 \tag{4.16}$$

as a measure of the effectiveness of receptivity.

To comply with the practice in experiments, we normalize the dimensional frequency of the T–S wave, ω_s^*, as

$$F = \omega_s^* \nu / U_\infty^2 \times 10^6,$$

which is related to $\hat{\omega}$ via

$$F = \hat{\omega} R^{-3/4} (T_w / T_\infty)^{-1} \times 10^6. \tag{4.17}$$

The Reynolds number is fixed at $R = 5 \times 10^5$ for which $\epsilon \approx 0.19$.

Figure 2 shows C_p as a function of the frequency F for $M = 0$ and $M = 0.8$, with the (physical) width of the suction slot being held constant: $(T_w/T_\infty)^{3/2} D = 4$. Both the first- and second-order results are included. As is illustrated, the receptivity is strong at the low-frequency end, and weakens as F increases. If one takes into account the subsequent development of the T–S wave, the most important frequency probably is centred at the neutral one, i.e. F_n as marked in the figure. This is because if the suction frequency is smaller than F_n, the T–S wave would decay before it eventually amplifies. On the other hand if the suction frequency is higher than F_n,

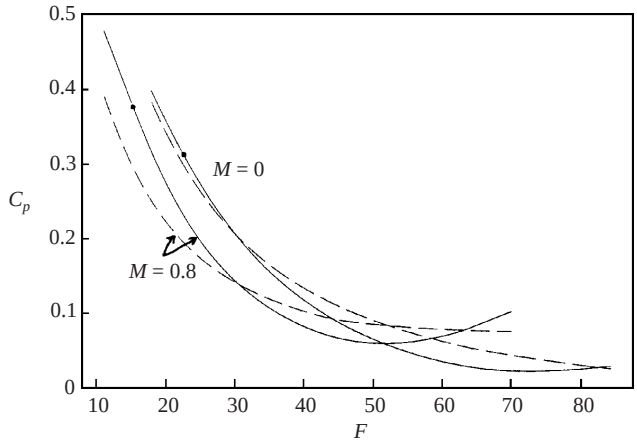

FIGURE 2. Variation of the coupling coefficient C_p with the suction frequency F for $M = 0,\ 0.8$. The solid lines: the second-order theory; the dashed lines: the 'first-order' theory. The neutral frequencies are marked by ●.

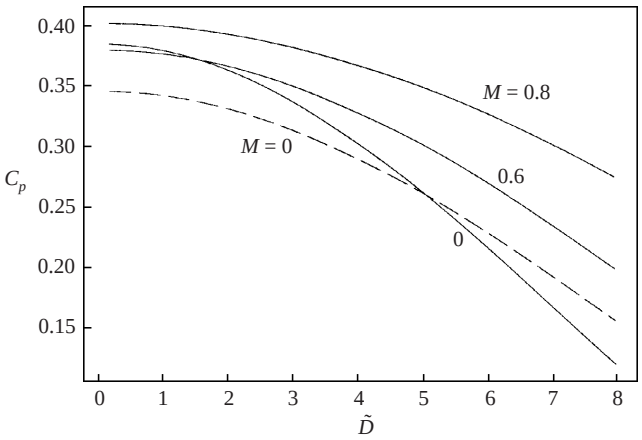

FIGURE 3. The variation of the coupling coefficient C_p with $\tilde{D} = (T_w/T_\infty)^{3/2}D$ for $M = 0,\ 0.8$. For each value of M, F is set to be the neutral frequency. The solid lines: the second-order theory; the dashed line: the 'first-order' theory for $M = 0$.

the T–S wave actually loses part of the exponentially growing region. In the major frequency range of interest (typically $F < 60$), the difference between first and second order is about 20%. Discrepancy of this order is broadly in line with experimental uncertainties. That the first- and second-order approximations are reasonably close gives us confidence in the reliability of the asymptotic results. However, at the higher frequency end, the difference could be more than 40%, in which case the theoretical prediction should be treated with great caution. A further examination indicates that the large discrepancy is due to the fact that the second-order correction to the eigenfunction, i.e. the expression in the square brackets in (4.6), becomes considerably larger than the leading-order approximation, the integral term in (4.6).

Figure 3 shows the variation of C_p with $\tilde{D} \equiv (T_w/T_\infty)^{3/2}D$ for three typical Mach numbers: $M = 0$, 0.6 and 0.8. For each value of M, the frequency F is taken to be the corresponding neutral frequency F_n. Clearly, a narrow suction slot is more effective

than a wide one, with the 'point' suction represented by the $D \to 0$ limit being most efficient. This limit is reached in practice when $\tilde{D} \approx 2$. For such a value, the width of the suction is approximately 1/10 the T–S wavelength.

5. Sound radiation

5.1. *The asymptotic behaviour of the pressure*

The solution for the pressure fluctuation in the upper deck can be written as

$$\tilde{p} = \epsilon^2 \left(\tilde{p}_1 + \epsilon \tilde{p}_2 + \epsilon^2 \tilde{p}_3 + \cdots\right), \tag{5.1}$$

where $\tilde{p}_1$, $\tilde{p}_2$ and $\tilde{p}_3$ are the Fourier inversions of $\bar{p}_1$, $\bar{p}_2$ and $\bar{p}_3$ respectively; see (3.26), (3.29) and (3.33). For instance,

$$\tilde{p}_1 = \frac{1}{(2\pi)^{1/2}} \int_{-\infty}^{\infty} \bar{P}_1(k)\, \mathrm{e}^{\mathrm{i}k\bar{x} - \bar{\kappa}\bar{y}}\, \mathrm{d}k. \tag{5.2}$$

In order to calculate the acoustic radiation, it is necessary to know the asymptotic behaviour of $\tilde{p}$ as $\bar{x}, \bar{y} \to \infty$. To that end, the integration path is now taken to be along the real axis. This is allowed when all the roots of Δ lie in the upper half-plane since the real axis is a causal contour. The solution so obtained will differ from the causal solution by $2\pi\mathrm{i}$ times the residue of the integrand when there is a root in the lower half-plane, but the latter part is exponentially small as $\bar{y} \to \infty$. Therefore in either case, deforming the causal contour to the real axis does not affect the far-field behaviour of the solution. It now follows that $\bar{\kappa} = |k|$. Since the phase of the integrand has no stationary point, the asymptotic behaviour of $\tilde{p}$ for large $\bar{x}$, $\bar{y}$ is determined by the nature of the integrand in the region near $k = 0$, implying that only small-wavenumber components of the near-field hydrodynamic motion are radiated into the sound, and this also occurs in the problem considered by Goldstein (1984*b*).

Note that $\zeta_0 \to \infty$ as $k \to 0$. It can be shown that

$$\int_{\zeta_0}^{\infty} \mathrm{Ai}(\zeta)\, \mathrm{d}\zeta / \mathrm{Ai}'(\zeta_0) \sim -\frac{1}{\zeta_0} \left(1 - \zeta_0^{-3/2} + O(\zeta_0)^{-3}\right). \tag{5.3}$$

Using this result in (3.49), (3.55) and (3.65) shows that as $k \to 0$

$$\bar{P}_1 \sim P_0 |k|, \quad \bar{P}_2 \sim -\frac{\omega(2 - M^2)P_0}{1 - M^2} \mathrm{sgn}(k), \quad \bar{P}_3 \sim \frac{(2 + M^2)\omega^2 P_0}{2(1 - M^2)^2} |k|^{-1}, \tag{5.4}$$

with

$$P_0 = -\frac{\mathrm{i}\widehat{V}_s(0)}{\hat{\omega}(1 - M^2)^{1/2}} = -(T_w/T_\infty)^{1/2} \frac{\mathrm{i}\widehat{V}_s(0)}{\omega(1 - M^2)^{1/2}}.$$

It then follows from Watson's lemma that as $\bar{r} = (\bar{x}^2 + \bar{y}^2)^{1/2} \to \infty$

$$\tilde{p}_1 \sim P_0 \frac{2[-\bar{x}^2 + (1 - M^2)\bar{y}^2]}{[\bar{x}^2 + (1 - M^2)\bar{y}^2]^2}, \tag{5.5}$$

$$\tilde{p}_2 \sim -\frac{(2 - M^2)\omega P_0}{1 - M^2} \frac{2\mathrm{i}\bar{x}}{\bar{x}^2 + (1 - M^2)\bar{y}^2} - M^2 \omega P_0 \frac{4\mathrm{i}\bar{x}\bar{y}^2}{[\bar{x}^2 + (1 - M^2)\bar{y}^2]^2}. \tag{5.6}$$

The third relation in (5.4) indicates that $\bar{P}_3$ should be understood as a generalized

function. The asymptote of $\tilde{p}_3$ is given by (see e.g. Lighthill 1964, p. 43),

$$\tilde{p}_3 \sim -\frac{(2+M^2)\omega^2 P_0}{(1-M^2)^2}\{\ln(\bar{x}^2+(1-M^2)\bar{y}^2)+\tilde{C}_3\}+\frac{M^4\omega^2 P_0}{(1-M^2)}\frac{\bar{y}^2[-\bar{x}^2+(1-M^2)\bar{y}^2]}{[\bar{x}^2+(1-M^2)\bar{y}^2]^2} + \frac{M^2(5-2M^2)\omega^2 P_0}{1-M^2}\frac{\bar{y}^2}{\bar{x}^2+(1-M^2)\bar{y}^2}, \quad (5.7)$$

where $\tilde{C}_3$ is an arbitrary constant; its appearance is merely a reflection of the fact that the Laplace equation admits the solution $\tilde{p}_3 = \text{constant}$ (cf. Crow 1970).

The far-field asymptotes of $\tilde{p}_1$, $\tilde{p}_2$ and $\tilde{p}_3$ indicate that they act respectively as quadrupole, dipole and monopole sources for the sound radiation. Although the latter two appear at higher orders in the upper deck, their contribution to the sound in the far field is as important as that of $\tilde{p}_1$. As was emphasized by Crighton (1992), such subtleties reflect the very essence of aeroacoustics.

Since the third term $\tilde{p}_3$ gives a monopole, which is an acoustic pole of the lowest order possible, there is no need to go further than $\tilde{p}_3$ (see e.g. Crow 1970; Crighton 1992). Mathematically, terms higher than $\tilde{p}_3$ would have the far-field asymptotes like $\bar{x}^m \log(\bar{x}^2+(1-M^2)\bar{y}^2)$ and $\bar{y}^m \log(\bar{x}^2+(1-M^2)\bar{y}^2)$ ($m \geqslant 1$). These seemingly unbounded terms would automatically match to the 'regular parts' in the small-distance asymptote of the acoustic solution.

5.2. *The acoustic field*

The asymptote of the pressure fluctuation in the upper deck implies that the expansion ceases to be valid when $\bar{x} = O(\epsilon^{-1})$ and $\bar{y} = O(\epsilon^{-1})$. This suggests the introduction of the variables

$$x^\dagger = \epsilon\bar{x}, \quad y^\dagger = \epsilon\bar{y}$$

to describe the acoustic field. The key difference from the upper deck is that the pressure fluctuation now satisfies the convected wave equation in a uniform stream,

$$M^2\left(-\mathrm{i}\omega+\frac{\partial}{\partial x^\dagger}\right)^2\tilde{p}-\left(\frac{\partial^2}{\partial x^{\dagger 2}}+\frac{\partial^2}{\partial y^{\dagger 2}}\right)\tilde{p}=0, \quad (5.8)$$

with the boundary condition that $\tilde{p} \to 0$ as $r^\dagger \equiv (x^{\dagger 2}+y^{\dagger 2})^{1/2} \to \infty$. A solution can be sought of the form

$$\tilde{p} = \frac{\epsilon^4}{\sqrt{2\pi}}p^\dagger(\hat{x},\hat{y})\mathrm{e}^{-\mathrm{i}M\hat{x}}, \quad (5.9)$$

where

$$\hat{x} = \frac{M\omega}{1-M^2}x^\dagger, \quad \hat{y} = \frac{M\omega}{(1-M^2)^{1/2}}y^\dagger \quad (5.10)$$

are renormalized coordinates. In terms of $(\hat{x},\hat{y})$, the governing equation for $p^\dagger$ reduces to the Helmholtz equation

$$\left(\frac{\partial^2}{\partial\hat{x}^2}+\frac{\partial^2}{\partial\hat{y}^2}\right)p^\dagger+p^\dagger=0,$$

so that we may express $p^\dagger$ as a superposition of multipoles:

$$p^\dagger = \left\{q_{11}\frac{\partial^2}{\partial\hat{x}^2}+q_{12}\frac{\partial^2}{\partial\hat{x}\hat{y}}+q_{22}\frac{\partial^2}{\partial\hat{y}^2}+d_1\frac{\partial}{\partial\hat{x}}+d_2\frac{\partial}{\partial\hat{y}}+m\right\}H_0^{(1)}(\hat{r}), \quad (5.11)$$

where $H_0^{(1)}$ denotes the Hankel function, and $\hat{r} = (\hat{x}^2 + \hat{y}^2)^{1/2}$. We may take $m = 0$ without losing generality since $H_0^{(1)}(\hat{r}) = -(\partial^2/\partial\hat{x}^2 + \partial^2/\partial\hat{y}^2)H_0^{(1)}(\hat{r})$. The remaining constants, q_{11}, q_{12}, q_{22}, d_1 and d_2, can be determined by matching with the upper-deck solution. To that end, we note that for small $\hat{r}$ (Abramowitz & Stegun 1964, p. 360)

$$H_0^{(1)}(\hat{r}) \sim \frac{2\mathrm{i}}{\pi}(1 - \tfrac{1}{4}\hat{r}^2)\ln\hat{r} + (1 - \tfrac{1}{4}\hat{r}^2) + \frac{2\mathrm{i}}{\pi} + \frac{2\mathrm{i}}{\pi}(\ln 2 + \gamma_E - 1)(1 - \tfrac{1}{4}\hat{r}^2) + \cdots, \quad (5.12)$$

with $\gamma_E \approx 0.5772$ being Euler's constant. Inserting (5.12) into (5.11) yields the small-$\hat{r}$ asymptote of the pressure fluctuation in the acoustic region, while the asymptote of the pressure in the upper deck as $\bar{r} = (\bar{x}^2 + \bar{y}^2)^{1/2} \to \infty$ can be obtained by substituting (5.5)–(5.7) into (5.1) and rewriting the resultant expression in terms of $\hat{x}$ and $\hat{y}$. On matching these two asymptotes, we find that

$$q_{11} = -\frac{\pi\mathrm{i}(1 + M^2)\omega^2 P_0}{(1 - M^2)^2}, \quad q_{22} = -\frac{\pi\mathrm{i}\omega^2 P_0}{(1 - M^2)^2}, \quad q_{12} = 0, \quad (5.13)$$

$$d_1 = -\frac{2\pi M\omega^2 P_0}{(1 - M^2)^2}, \quad d_2 = 0. \quad (5.14)$$

Inserting these constants into (5.11) and making use of the fact that $H_0^{(1)}(\hat{r}) \sim \sqrt{2/\pi}\,\hat{r}^{-1/2}\mathrm{e}^{\mathrm{i}(\hat{r} - \pi/4)}$ for large $\hat{r}$, we find that as $\hat{r} \to \infty$,

$$\tilde{p} \sim (T_w/T_\infty)^{1/2}\frac{\epsilon^4\omega\widehat{V}_s(0)}{(1 - M^2)^{7/4}}\frac{q(\theta, M)}{(M\omega r^\dagger)^{1/2}} \times \exp\left\{\mathrm{i}\left(\frac{M\omega(1 - M^2\sin^2\theta)^{1/2}}{1 - M^2}r^\dagger - \frac{M\omega}{1 - M^2}x^\dagger - \frac{\pi}{4}\right)\right\} \quad (5.15)$$

where the directivity function $q(\theta, M)$ is given by

$$q(\theta, M) = \frac{(1 - M^2)^{1/4}}{(1 - M^2\sin^2\theta)^{1/4}}\left[1 - \frac{M\cos\theta}{(1 - M^2\sin^2\theta)^{1/2}}\right]^2, \quad (5.16)$$

with θ being the observation angle (see figure 1).

To facilitate the interpretation of the result (5.15), we introduce the coordinates (x_d, y_d) normalized by d^*, as well as the time variable t_d normalized by d^*/U_∞, where d^* is the width of the suction slot. Suppose that in terms of x_d the suction velocity is given by $(v_s(x_d)\mathrm{e}^{\mathrm{i}\omega_d t_d} + \text{c.c.})$, and the Fourier transform of $v_s(x_d)$ with respect to x_d is $\widehat{v}_s(k)$, where ω_d denotes the frequency normalized by U_∞/d^*. Then the following relations hold:

$$(x^\dagger, y^\dagger) = \epsilon^{-2}K^{-1}(d^*/L)(x_d, y_d), \quad \omega = \epsilon^2 K(d^*/L)^{-1}\omega_d,$$

$$\widehat{V}_s(0) = \epsilon^{-6}(T_w/T_\infty)^{-1/2}K^{-1}(d^*/L)\widehat{v}_s(0).$$

After performing the above substitutions in (5.15), it can be shown that

$$\tilde{p} \sim \frac{\omega_d\widehat{v}_s(0)}{(1 - M^2)^{7/4}}\frac{q(\theta, M)}{(M\omega r_d)^{1/2}} \times \exp\left\{\mathrm{i}\left(\frac{M\omega_d(1 - M^2\sin^2\theta)^{1/2}}{1 - M^2}r_d - \frac{M\omega_d}{1 - M^2}x_d - \frac{\pi}{4}\right)\right\} \quad (5.17)$$

where $r_d = (x_d^2 + y_d^2)^{1/2}$.

The final result (5.17) exhibits no explicit dependence on the profile of the mean flow, nor on the wall friction or temperature. However it would be wrong to conclude that the shear plays no role in the sound radiation. To see this point, let us consider the purely inviscid model where the mean flow is replaced by a uniform stream. The pressure $\tilde{p}_I$ is then governed by the equation

$$M^2\left(-\mathrm{i}\omega_d+\frac{\partial}{\partial x_d}\right)^2\tilde{p}_I-\left(\frac{\partial^2}{\partial x_d^2}+\frac{\partial^2}{\partial y_d^2}\right)\tilde{p}_I=0, \tag{5.18}$$

subject to the boundary condition

$$\frac{\partial\tilde{p}_I}{\partial y_d}=-\left(-\mathrm{i}\omega_d+\frac{\partial}{\partial x_d}\right)v_s(x_d)\quad\text{at}\quad y_d=0. \tag{5.19}$$

The system (5.18)–(5.19) can be easily solved by using the Fourier transform to obtain

$$\tilde{p}_I=\frac{\mathrm{i}}{\sqrt{2\pi}}\int_{-\infty}^{\infty}\frac{(k-\omega_d)\widehat{v}_s(k)}{[k^2-M^2(k-\omega_d)^2]^{1/2}}\exp\{\mathrm{i}kx_d-[k^2-M^2(k-\omega_d)^2]^{1/2}y_d\}\,\mathrm{d}k.$$

The above integral has a stationary phase point at

$$k_s=\frac{M\omega_d}{1-M^2}\left(-M+\frac{\cos\theta}{(1-M^2\sin^2\theta)^{1/2}}\right),$$

and the method of stationary phase shows that as $r_d=(x_d^2+y_d^2)^{1/2}\to\infty$,

$$\tilde{p}_I\sim\frac{\omega_d\widehat{v}_s(k_s)}{(1-M^2)^{7/4}}\frac{q_0(\theta,M)}{(M\omega_d r_d)^{1/2}}\times\exp\left\{\mathrm{i}\left(\frac{M\omega_d(1-M^2\sin^2\theta)^{1/2}}{1-M^2}r_d-\frac{M\omega_d}{1-M^2}x_d-\frac{\pi}{4}\right)\right\}, \tag{5.20}$$

where

$$q_0(\theta,M)=\frac{(1-M^2)^{1/4}}{(1-M^2\sin^2\theta)^{1/4}}\left[1-\frac{M\cos\theta}{(1-M^2\sin^2\theta)^{1/2}}\right], \tag{5.21}$$

and $\widehat{v}_s(k_s)\approx\widehat{v}_s(0)$ since $\omega_d=\epsilon\omega_s$.

It can seen that (5.17) and (5.20) have the same multiplicative factor, but the directivity functions predicted by the triple-deck and inviscid models are different. Such a difference is not totally surprising since the triple-deck structure, though fairly insensitive to the detailed profile, requires the mean flow to vanish at the wall, a property not possessed by a uniform flow.

In figure 4, we plot the directivity (5.16) at three Mach numbers. Interestingly, the emission is beamed to the upstream direction. Such a feature is also predicted by the purely inviscid solution (5.21), but is much less significant than that shown in figure 4.

6. Conclusions and discussions

By analysing a relatively simple flow, namely a subsonic boundary layer subject to unsteady suction, we have demonstrated an asymptotic procedure for determining the acoustic field of an unsteady triple-deck flow. In this approach, the source and the sound can be calculated in a systematic way. Another aspect considered is the generation of instability waves, i.e. the receptivity problem. The amplitudes of these

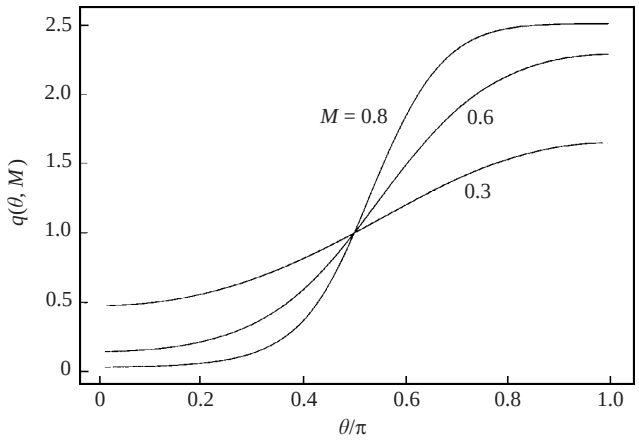

FIGURE 4. The directivity of the acoustic far field.

waves are fully determined, and their presence does not cause indeterminacy. The radiation and receptivity are two processes taking place simultaneously, both of which have been adequately described by the present approach.

It is well known that Lilley's equation may admit eigensolutions corresponding to instability waves, a feature that sometimes has been held against Lilley's analogy (see e.g. Howe 1975; Ffowcs Williams 1977). Some authors choose to suppress the instability waves in favour of a bounded solution. Such a treatment violates strict causality, but does not affect the acoustic field in the case of doubly infinite vortex sheet (Mani 1976; Dowling *et al.* 1978), since the homogeneity in the streamwise direction means that the Kelvin–Helmholtz instability waves are nowhere coupled to the sound. However, in the more complex situation where some form of discontinuity (e.g. an edge) is present, it is recognized that instability waves may be a significant source of sound. An arbitrary prescription of the instability waves downstream the edge without considering the external perturbations may result in misleading prediction of the sound radiation (cf. Crighton 1972*a*; Howe 1976). Unfortunately, the determination of the instability waves can be difficult within the context of pure acoustic analogy, because some vital hydrodynamic aspects of the problem are not always contained in the acoustic tensor. To resolve fully the receptivity, one has to go beyond the framework of acoustic analogy.

The method presented in this paper can be used to solve a range of problems where the acoustic sources are associated with triple-deck flows. For example, since T–S waves are described by triple-deck structure, our approach can immediately be used to analyse the acoustic radiation as an oncoming T–S wave interacts with some form of rapidly varying mean flow (caused e.g. by a local roughness element). This is being currently pursued, but the most important application that we have in mind is to the trailing-edge noise, for which various theories have been proposed (see Howe 1978). In particular, it has been suggested that the turbulence in the boundary layer, when passing the edge, may be diffracted into sound. Such a process was first investigated by Ffowcs Williams & Hall (1970), who solved Lighthill's acoustic analogy equation for the case of a half-plane immersed in a turbulent flow. The source was represented by Lighthill's quadrupoles, and the mean flow was absent. Howe (1976) developed a theory in which the turbulence is represented by a convected line vortex (or gust), and the shear layer by a semi-infinite vortex sheet. Remarkably, his analysis shows that if the Kutta condition is imposed and the vortex moves with

the free-stream velocity, the sound generated by the gust cancels the sound produced by shed vorticity in the wake, with the consequence that there is no net sound being emitted. Howe then suggests that any edge sound must be produced due to some nonlinear effects. There is however another possibility: that is, near the trailing edge the mean flow is rapidly varying and is governed by triple-deck theory. Turbulence may interact with this flow to produce sound. Another source of trailing-edge noise is the diffraction of the oncoming T–S waves, as has been suggested by experimental evidence (e.g. Arbey & Bataille 1983; Nash & Lowson 1999). Investigations thus far still stay at the level of correlating the spectra of the sound field and instability waves, and there has been no first-principle analysis aimed at direct calculation of the sound. This process certainly cannot be modelled by a semi-infinite vortex sheet because the uniform stream over the plate supports no instability waves, although Kelvin–Helmholtz instability waves develop on the vortex sheet. To take account of the oncoming T–S waves that develop in the upstream boundary layer, the local triple-deck flow has to be an important part of the model. It appears to us that the approach developed in the present work may provide a basic framework for tackling the above two problems.

Finally it may be worth pointing out that while the relevance of triple-deck theory to aeroacoustics is well known (e.g. Crighton 1985; Peake 1994), its role so far has been limited to providing a justification for imposing the Kutta condition on inviscid solutions. The present work seems to be the first that integrates the triple-deck structure into an overall scheme for predicting the sound radiation.

The author would like to thank Professors J. T. Stuart, D. W. Moore, F. G. Leppington, H. Zhou and M. Gaster, and Dr S. J. Cowley for helpful discussions and comments. The referees are thanked for their detailed comments and suggestions, which have led to improvement of the work.

Appendix. Definitions of integrals

$$I_1 = \int_0^\infty (R_B U_B - 1)\,\mathrm{d}\tilde{y}, \tag{A 1}$$

$$I_2 = \int_0^\infty (R_B U_B^2 - 1)\,\mathrm{d}\tilde{y}, \tag{A 2}$$

$$J_0 = \tilde{a}M^2 - \int_0^{\tilde{a}} \left(\frac{1}{R_B U_B^2} - T_w/T_\infty \frac{1}{\lambda^2 \tilde{y}^2} \right) \mathrm{d}\tilde{y} + T_w/T_\infty \frac{1}{\lambda^2 \tilde{a}}, \tag{A 3}$$

$$J_\infty = \int_{\tilde{a}}^\infty \left(\frac{1}{R_B U_B^2} - 1 \right) \mathrm{d}\tilde{y} - (1 - M^2)\tilde{a}\ ; \tag{A 4}$$

$$\begin{aligned} H_3 = {} & \int_0^{\tilde{a}} R_B U_B^2 \left\{ \int_{\tilde{a}}^{\tilde{y}} \frac{\mathrm{d}\tilde{y}_1}{R_B U_B^2} \right\} \mathrm{d}\tilde{y} + \left\{ \int_{\tilde{a}}^\infty \left(\frac{1}{R_B U_B^2} - 1 \right) \mathrm{d}\tilde{y} \right\} \left\{ \int_{\tilde{a}}^\infty (R_B U_B^2 - 1)\,\mathrm{d}\tilde{y} - \tilde{a} \right\} \\ & + \int_{\tilde{a}}^\infty (R_B U_B^2 - 1)(\tilde{y} - \tilde{a})\,\mathrm{d}\tilde{y} - \int_{\tilde{a}}^\infty R_B U_B^2 \left\{ \int_{\tilde{y}}^\infty \left(\frac{1}{R_B U_B^2} - 1 \right) \mathrm{d}\tilde{y}_1 \right\} \mathrm{d}\tilde{y} + \tfrac{1}{2}\tilde{a}^2 \\ & - M^2 \int_0^\infty (R_B U_B^2 - 1)(\tilde{y} - \tilde{a})\,\mathrm{d}\tilde{y}, \end{aligned} \tag{A 5}$$

$$H_5 = \int_0^\infty \left(\frac{1}{R_B U_B^2} - 1\right) \left\{ \int_0^{\tilde{y}} R_B U_B^2 \, \mathrm{d}\tilde{y}_1 \right\} \mathrm{d}\tilde{y} - (1 - M^2) \int_0^\infty \tilde{y}(R_B U_B^2 - 1) \, \mathrm{d}\tilde{y}, \quad \text{(A 6)}$$

$$H_6^\infty = 2 \int_{\tilde{a}}^\infty \left(\frac{1}{R_B U_B^3} - 1\right) \mathrm{d}\tilde{y} - \int_{\tilde{a}}^\infty \left(\frac{1}{R_B U_B^2} - 1\right) \mathrm{d}\tilde{y} - (1 + M^2)\tilde{a}, \quad \text{(A 7)}$$

$$H_6^0 = -2 \int_0^{\tilde{a}} \left(\frac{1}{U_B^3} - T_w/T_\infty \frac{1}{\lambda^3 \tilde{y}^3} + \frac{(\gamma - 1)M^2}{\lambda \tilde{y}}\right) \mathrm{d}\tilde{y}$$

$$+ T_w/T_\infty \frac{1}{\lambda^3 \tilde{a}^2} + \frac{(\gamma - 1)M^2}{\lambda} (2 \ln \tilde{a} - \tfrac{4}{3}). \quad \text{(A 8)}$$

In all the expressions above, the parameter $\tilde{a}$ is arbitrary provided $\tilde{a} \neq 0$. Since the Blasius profile U_B is a function of the similarity variable $\eta \sim (1 + x)^{-1/2}$, it is convenient, when evaluating these integrals, to choose $\tilde{a} = a_0(1 + x)^{1/2}$ with a_0 being independent of x.

REFERENCES

Abramowitz, M. & Stegun, I. A. 1964 *Handbook of Mathematical Functions*. National Bureau of Standards.

Arbey, H. & Bataille, J. 1983 Noise generated by airfoil placed in a uniform laminar flow. *J. Fluid Mech.* **134**, 33–47.

Ashpis, D. E. & Reshotko, E. 1990 The vibrating ribbon problem revisited. *J. Fluid Mech.* **213**, 531–547.

Bodonyi, R. J. & Duck, P. W. 1992 Boundary-layer receptivity due to a wall suction and control of Tollmien-Schlichting waves. *Phys. Fluids* **4**, 1204–1214.

Crighton, D. G. 1972*a* Radiation properties of the semi-infinite vortex sheet. *Proc. R. Soc. Lond.* A **330**, 185–198.

Crighton, D. G. 1972*b* The excess noise field of subsonic jet. *J. Fluid Mech.* **56**, 683–694.

Crighton, D. G. 1981 Acoustics as a branch of fluid mechanics. *J. Fluid Mech.* **106**, 261–298.

Crighton, D. G. 1985 The Kutta condition in unsteady flow. *Annu. Rev. Fluid Mech.* **17**, 411–445.

Crighton, D. G. 1992 Matched asymptotic expansions applied to acoustics. In *Modern Methods in Analytical Acoustics: Lecture Notes* (ed. D. G. Crighton, A. G. Dowling, M. Heckl & F. G. Leppington). Springer.

Crighton, D. G. & Leppington, F. G. 1971 On the scattering of aerodynamics noise. *J. Fluid Mech.* **46**, 577–597.

Crighton, D. G. & Leppington, F. G. 1973 Singular perturbation methods in acoustics: diffraction by a plate of finite thickness. *Proc. R. Soc. Lond.* A **335**, 313–339.

Crow, S. C. 1970 Aerodynamic sound emission as a singular perturbation problem. *Stud. Appl. Maths* **49**, 21–44.

Dietz, A. J. 1999 Local boundary-layer receptivity to a convected free-stream disturbance. *J. Fluid Mech.* **378**, 291–317.

Dowling, A. P., Ffowcs Williams, J. E. & Goldstein, M. E. 1978 Sound generation in a moving stream. *Phil. Trans. R. Soc. Lond.* A **288**, 321–349.

Duck, P. W., Ruban, A. I. & Zhikharev, C. N. 1996 Generation of Tollmien-Schlichting waves by free-stream turbulence. *J. Fluid Mech.* **312**, 341–371.

Ffowcs Williams, J. E. 1974 Sound production at the edge of a steady flow. *J. Fluid Mech.* **66**, 791–816.

Ffowcs Williams, J. E. 1977 Aeroacoustics. *Annu. Rev. Fluid Mech.* **9**, 447–468.

Ffowcs Williams, J. E. & Hall, L. H. 1970 Aerodynamic sound generation by turbulent flow in the vicinity of a scattering half-plane. *J. Fluid Mech.* **40**, 657–670.

Gaster, M. 1965 On the generation of spatially growing waves in a boundary layer. *J. Fluid Mech.* **22**, 433–441.

Goldstein, M. E. 1976 *Aeroacoustics*. McGraw-Hill.

GOLDSTEIN, M. E. 1984*a* Aeroacoustic of turbulent shear flows. *Annu. Fluid Mech.* **16**, 263–285.

GOLDSTEIN, M. E. 1984*b* Sound generation and upstream influence due to instability wave interacting with non-uniform mean-flows. *J. Fluid Mech.* **149**, 161–177.

GOLDSTEIN, M. E. 1985 Scattering of acoustic waves into Tollmien-Schlichting waves by small streamwise variations in surface geometry. *J. Fluid Mech.* **154**, 509–529.

HOWE, M. S. 1975 Contributions to the theory of aerodynamics sound, with application to excess jet noise and the theory of the flute. *J. Fluid Mech.* **71**, 625–673.

HOWE, M. S. 1976 The influence of vortex shedding on the generation of sound by convected turbulence. *J. Fluid Mech.* **76**, 711–740.

HOWE, M. S. 1978 A review of theory of trailing edge noise. *J. Sound Vib.* **61**, 437–465.

KAMBE, T. 1986 Acoustic emissions by vortex motions. *J. Fluid Mech.* **173**, 643–666.

LIGHTHILL, M. J. 1952 On sound generated aerodynamically. *Proc. R. Soc. Lond.* A **211**, 564–587.

LIGHTHILL, M. J. 1954 On sound generated aerodynamically. II. Turbulence as a source of sound. *Proc. R. Soc. Lond.* A **222**, 1–32.

LIGHTHILL, M. J. 1964 *An Introduction to Fourier Analysis and Generalised Functions.* Cambridge University Press.

LILLEY, G. M. 1974 On the noise from jets, noise mechanisms. *AGARD-CP*-131, pp. 13.1–13.12.

MANI, R. 1976 The influence of jet flow on jet noise. Part I. The noise of unheated jets. *J. Fluid Mech.* **73**, 753–778.

NASH, E. C. & LOWSON, M. V. 1999 Boundary-layer instability noise on airfoils. *J. Fluid Mech.* **382**, 27–61.

OBERMEIER, F. 1967 Berechnung aerodynamisch erzeugter Schallfelder mittels der Mthode der 'Matched Asymptotic Expansions'. *Acustica* **18**, 238–240.

PEAKE, N. 1994 The viscous interaction between sound waves and the trailing edge of a supersonic splitter plate. *J. Fluid Mech.* **264**, 321–342.

PHILLIPS, O. M. 1960 On the generation of sound by supersonic turbulent shear layer. *J. Fluid Mech.* **9**, 1–28.

RUBAN, A. I. 1984 On Tollmien-Schlichting wave generation by sound. *Izv. Akad. Nauk. SSSR Mekh. Zhid. Gaza* **5**, 44 (in Russian; English transl. *Fluid Dyn.* **19**, 709–716, (1985)).

SMITH, F. T. 1979 On the nonparallel flow stability of the Blasius boundary layer. *Proc. R. Soc. Lond.* A **366**, 91–109.

SMITH, F. T. 1989 On the first-mode instability in subsonic, supersonic or hypersonic boundary layers. *J. Fluid Mech.* **198**, 127–153.

STEWARTSON, K. 1974 Multistructured boundary layers on flat plates and related bodies. *Adv. Appl. Mech.* **14**, 145–239.

TAM, C. K.W. 1998 Mean-flow refraction effects on sound radiated from localized sources in a jet. *J. Fluid Mech.* **370**, 149–174.

TERENT'EV, E. D. 1981 The linear problem of a vibrator in a subsonic boundary layer. *Prikl. Math. Mech.* **45**(6), 1049–1055.

TERENT'EV, E. D. 1984 The linear problem of a vibrator performing harmonic oscillation at super-critical frequencies in a subsonic boundary layer. *Prikl. Math. Mech.* **48**(2), 184–191.

WU, X. 1999 Generation of Tollmien-Schlichting waves by convecting gusts interacting with sound. *J. Fluid Mech.* **397**, 285–316.

WU, X. 2001*a* Receptivity of boundary layers with distributed roughness to acoustical and vortical disturbances: a second-order theory and comparison with experiments. *J. Fluid Mech.* **431**, 91–133.

WU, X. 2001*b* On local boundary-layer receptivity to vortical disturbances in the free stream. *J. Fluid Mech.* **449**, 373–393.